

Cobomarsen, an oligonucleotide inhibitor of miR-155, co-ordinately regulates multiple survival pathways to reduce cellular proliferation and survival in cutaneous T-cell lymphoma

Anita G. Seto,^{1,*} Xuan Beatty,¹ Joshua

M. Lynch,¹ Melanie Hermreck,¹

Michael Tetzlaff,² Madeleine Duvic³

and Aimee L. Jackson¹ 

¹miRagen Therapeutics, Inc., Boulder, CO,

²Section of Dermatopathology, Department of Pathology, Department of Translational and Molecular Pathology, The University of Texas MD Anderson Cancer Center, and ³Department of Dermatology, The University of Texas MD Anderson Cancer Center, Houston, TX, USA

Received 17 April 2018; accepted for publication 19 June 2018

Correspondence: Aimee L. Jackson, miRagen Therapeutics, Inc., 6200 Lookout Road, Boulder, CO 80301, USA.

E-mail: ajackson@miragen.com

*Current address: Expansion Therapeutics, Inc., San Diego, CA, USA

This work was presented, in part, at the 57th Annual Meeting of the American Society of Hematology, Orlando, FL, December 2015.

Summary

miR-155, a microRNA associated with poor prognosis in lymphoma and leukaemia, has been implicated in the progression of mycosis fungoides (MF), the most common form of cutaneous T-cell lymphoma (CTCL). In this study, we developed and tested cobomarsen (MRG-106), a locked nucleic acid-modified oligonucleotide inhibitor of miR-155. In MF and human lymphotropic virus type 1 (HTLV-1+) CTCL cell lines *in vitro*, inhibition of miR-155 with cobomarsen de-repressed direct miR-155 targets, decreased expression of multiple gene pathways associated with cell survival, reduced survival signalling, decreased cell proliferation and activated apoptosis. We identified a set of genes that are significantly regulated by cobomarsen, including direct and downstream targets of miR-155. Using clinical biopsies from MF patients, we demonstrated that expression of these pharmacodynamic biomarkers is dysregulated in MF and associated with miR-155 expression level and MF lesion severity. Further, we demonstrated that miR-155 simultaneously regulates multiple parallel survival pathways (including JAK/STAT, MAPK/ERK and PI3K/AKT) previously associated with the pathogenesis of MF, and that these survival pathways are inhibited by cobomarsen *in vitro*. A first-in-human phase 1 clinical trial of cobomarsen in patients with CTCL is currently underway, in which the panel of proposed biomarkers will be leveraged to assess pharmacodynamic response to cobomarsen therapy.

Keywords: cutaneous T-cell lymphoma, miR-155, cobomarsen, mycosis fungoides, Sézary syndrome.

MicroRNAs, short (~22 nt) non-coding RNAs that regulate post-transcriptional gene expression, are potential therapeutic targets in cancer (Lin & Gregory, 2015). Through homologous base pairing with the 3' untranslated regions (UTRs) of specific mRNA targets, microRNAs can promote mRNA degradation and inhibit translation (Bartel, 2009). More than one-third of human genes are predicted to be targets of microRNA control (Lewis *et al*, 2005). A single microRNA might coordinately regulate a network of genes encoding proteins with related functions (e.g., cellular proliferation or metabolism) (Stark *et al*, 2003; Grün *et al*, 2005; Lewis *et al*, 2005; Linsley *et al*, 2007).

The microRNA miR-155 regulates immune cell function and is overexpressed in numerous solid tumours and haematological malignancies (Eis *et al*, 2005; Kluiver *et al*, 2005;

Tili *et al*, 2011). Constitutively high levels of miR-155 resulted in sustained cell proliferation and survival (Wang & Lee, 2009; Yamanaka *et al*, 2009; Gerloff *et al*, 2015) and genomic instability of malignant cells (Valeri *et al*, 2010; Babar *et al*, 2011; Tili *et al*, 2011). Additionally, multiple studies of genetically manipulated mice have demonstrated that overexpression of the murine homologue of miR-155 in select lymphoid tissues or cell types can lead to an increased incidence of lymphomas and leukaemias (Metzler *et al*, 2004; Eis *et al*, 2005; Costinean *et al*, 2006; O'Connell *et al*, 2008; Babar *et al*, 2012). Together, these results suggest that miR-155 might play a role in the genesis and/or proliferation of haematological malignancies.

In particular, miR-155 has been implicated in some subtypes of cutaneous T-cell lymphoma (CTCL), a clinically

heterogeneous group of T cell-derived lymphoproliferative malignancies that home to the skin. Mycosis fungoides (MF), the most prevalent subtype of CTCL, can remain indolent or progress from limited patches and plaques in the epidermis to tumour formation in some patients (Willemze *et al*, 2013). Many groups have reported overexpression of miR-155 in skin biopsies from patients with advanced MF compared with controls (van Kester *et al*, 2011; Ralfkiaer *et al*, 2011, 2014; Moyal *et al*, 2013; Marosvari *et al*, 2015; Sandoval *et al*, 2015; Garaicoa *et al*, 2016), which suggests that miR-155 might play a role in disease progression of MF (Kopp *et al*, 2013a; Moyal *et al*, 2013, 2017). In fact, the measurement of miR-155 together with two other microRNAs (miR-203 and miR-205) has been proposed as a diagnostic tool for MF (Ralfkiaer *et al*, 2011; Marstrand *et al*, 2014). In contrast, miR-155 was not highly upregulated in peripheral blood CD4⁺ cells isolated from patients with Sézary syndrome (SS), an aggressive leukaemic subtype of CTCL (Ballabio *et al*, 2010; Narducci *et al*, 2011; Qin *et al*, 2012).

Several mechanistic studies suggest that the effects of miR-155 in CTCL are mediated through activation of survival pathways. In cultured MF cell lines, miR-155 overexpression has been linked to constitutive activation of the JAK/STAT, NF-κB and PI3K/AKT survival pathways (Ma *et al*, 2011; Huang *et al*, 2012; Kopp *et al*, 2013a; Rasmussen *et al*, 2015). Activation of these pathways in response to stimulation of the T-cell receptor has been shown to result in increased miR-155 expression (Rincon *et al*, 2001; So & Fruiman, 2012; Seif *et al*, 2017). In addition, the direct targets of miR-155 include genes that negatively regulate signalling through these pathways (O'Connell *et al*, 2009; Viernes *et al*, 2014; Yang *et al*, 2015a,b). Finally, dysregulation of these survival pathways has been shown to be important in the pathogenesis and progression of CTCL (Izban *et al*, 2000; Qin *et al*, 2001; Tracey *et al*, 2004; Sors *et al*, 2006; Kopp *et al*, 2013a; Litvinov *et al*, 2013, 2014; Wang *et al*, 2015). However, it is not clear whether miR-155 overexpression can promote the malignant phenotype of MF by triggering signalling through these pathways. Nor is it known whether survival pathways regulated by miR-155 are dysregulated in clinical MF biopsies, and whether pathway activation correlates with miR-155 expression and MF disease severity. The studies described here elucidate the mechanism of miR-155 in MF using an inhibitor of miR-155 in cell-based systems and through the analysis of cells and clinical specimens with whole transcriptome profiling.

We developed cobomarsen (MRG-106), an oligonucleotide inhibitor of miR-155 optimized for functional uptake in CD4⁺ T cells and MF cells. Using this inhibitor, we wanted to identify pharmacodynamic biomarkers of miR-155 inhibition for translation into the clinical setting. We hypothesized that these biomarkers might be dysregulated in clinical MF biopsies and that their dysregulated expression correlates with miR-155 and lesion severity. Further, we hypothesized

that inhibition of miR-155 with cobomarsen could reverse the malignant phenotype of MF by restoring the normal expression and function of multiple coordinated gene networks that control survival signalling and apoptosis.

Methods

Cell lines, cell culture and treatments

Five commercially-available human-derived T lymphocyte cell lines were used in this study: MF cell line My-La (catalogue number 95051032; Sigma-Aldrich, St Louis, MO, USA), HTLV-1+ CTCL cell lines HuT 102 (ATCC® TIB-162™; American Type Culture Collection [ATCC], Manassas, VA, USA) and MJ [G11] (ATCC® CRL8294™), SS cell line HuT 78 (ATCC® TIB-161™) and unspecified CTCL cell line HH (ATCC® CRL2105™). RPMI-1640 medium and Iscove's modified Dulbecco's medium (IMDM) were purchased from ATCC, fetal bovine serum (FBS) from ThermoFisher Scientific (Waltham, MA, USA), glutamine from Lonza (Walkersville, MD, USA) and human interleukin (IL) 2, IL4, and AB serum from Sigma-Aldrich. Cell lines were seeded at 200 000 cells/ml and passaged before reaching a density of 1×10^6 cells/ml. Treatments included bexarotene (Sigma-Aldrich) and small molecule inhibitors idelalisib (PI3K/AKT inhibitor), ruxolitinib (JAK/STAT inhibitor) and U0126-EtOH (MAPK/ERK inhibitor) (all Selleckchem, Houston, TX, USA).

CD4⁺ T cells were isolated from peripheral blood mononuclear cells (PBMCs) of healthy donors using magnetic bead separation (CD4⁺ T cell isolation kit; Miltenyi Biotec, Auburn, CA, USA) according to the manufacturer's instructions. Isolated CD4⁺ T cells were cultured at a density of 1×10^6 cells/ml in complete RPMI medium (supplemented with HEPES, NEAA, Na Pyruvate, Pen Strep and 2-ME) containing 10% FBS. Cells were stimulated using anti-CD3/anti-CD28-coated Dynabeads™ (ThermoFisher Scientific) at a 1:1 ratio in the presence of 50 U/ml recombinant human IL-2 (PeproTech, Rocky Hill, NJ, USA). Cobomarsen or small molecule inhibitors were added at the time of stimulation and cells were cultured for 2 days.

For passive oligonucleotide uptake, treatments were added directly to the growth medium without the addition of transfection agents or additives, for up to 12 days. For nucleofection, cells were transfected using Amaxa Cell Line Nucleofector Kit L (Lonza) following the manufacturer's protocol. Briefly, approximately 2×10^6 cells were transfected using program Q-100 on the Amaxa Nucleofector II device, subsequently plated in 96-well plates in triplicate, and harvested at 24 and 48 h for molecular assessments.

Oligonucleotides

Single-stranded oligonucleotides were chemically synthesized and purified by miRagen Therapeutics (Boulder, CO, USA)

under non-good manufacturing practice conditions. An inhibitor targeting a *Caenorhabditis elegans* microRNA not expressed in mammals was used as a control.

RNA extraction from cells

Total RNA containing small RNAs was extracted using RNeasy (Qiagen, Germantown, MD, USA). RNA isolated from human normal peripheral blood CD4+ helper T cells was purchased from AllCells (Alameda, CA, USA).

Quantitative real-time polymerase chain reaction (qRT-PCR) analysis of gene and microRNA expression

Twenty nanograms of total RNA were reverse transcribed with MultiScribeTM reverse transcriptase (ThermoFisher Scientific), according to the manufacturer's instructions. Gene and microRNA expression were measured with TaqMan[®] assays (ThermoFisher Scientific). Expression was normalized to a housekeeping gene or small RNA, as appropriate, and calculated as relative expression compared to the average of the control group. To determine miR-155 copy number, standard curves were generated using a synthetic miR-155 RNA template (ThermoFisher Scientific). miR-155 copy number per cell was extrapolated from the standard curves, assuming 10 pg of total RNA per cell.

Assays for cellular adenosine triphosphate (ATP) and caspase 3/7 activity

Cellular ATP concentration, which correlates linearly with total cell number (data not shown), was measured with the CellTiter-Glo luminescent cell viability assay (Promega, Madison, WI, USA), according to the manufacturer's instructions. Cellular caspase 3/7 activity, a surrogate measure of apoptosis, was measured with the Caspase-Glo 3/7 assay system (Promega), according to the manufacturer's instructions. Luminescence was measured on a Synergy HT plate reader (BioTek Instruments, Winooski, VT, USA) and normalized to the result for untreated cells at 24 h. Luminescence of caspase 3/7 was also normalized to the corresponding ATP signal, because growing cells have a low basal level of caspase activity.

Microarray analysis

Cutaneous T-cell lymphoma cell lines were cultured with cobomarsen for 4 days (to identify direct targets) or 8 days (to identify downstream targets). RNA was extracted with miRNeasy mini kits (Qiagen), according to the manufacturer's instructions. The Affymetrix GeneChip Human Genome U133 Plus 2.0 array was run by Expression Analysis, Inc. (Durham, NC, USA). Affymetrix .chp files were analysed using OmicSoft Array Studio software (Cary, NC, USA). Raw microarray data is available on the NCBI Gene

Expression Omnibus GSE112273 (<https://www.ncbi.nlm.nih.gov/geo/query/acc.cgi?acc=GSE112273>). Quality of the arrays was confirmed by principal component analysis. To identify differentially regulated genes, a one-way ANOVA test was performed to compare cobomarsen-treated to untreated samples for the corresponding cell line. Significantly regulated genes were defined using a Benjamini-Hochberg false discovery rate (BH-FDR) corrected *P*-value cut-off of ≤ 0.05 to control for multiple testing. Genes were defined as detectable if they were present in more than two of the four replicates for a given treatment. Hierarchical clustering was performed using the software program R (<https://www.r-project.org/>) using an agglomerative metric with Euclidean distance. Enrichment for seed-matched genes was determined by the overlap of the cobomarsen signature with the Ensembl Gene IDs on the Affymetrix array that contain a miR-155 seed complementary sequence (heptamer or octamer) in their 3' UTR. Enrichment for functional annotation was determined by two approaches. First, the differentially regulated genes were assessed using the functional annotation tool on the DAVID Bioinformatics Resources website (<http://david.abcc.ncifcrf.gov/>). Functional annotation clusters were generated using gene ontology (GO) biological process and GO molecular function terms. Enriched terms were defined as those with a BH-FDR *P* < 0.01 . Second, the hypergeometric *P*-value was calculated for overlap between the cobomarsen signature gene lists and gene lists for the functional terms APOPTOSIS_GO (GO:0006915) and CELL_CYCLE_GO_0007049 (GO:0007049), which were extracted from the Broad Institute MSigDB Molecular Signatures Database (<http://www.broadinstitute.org/gsea/msigdb/index.jsp>).

Flow cytometric analysis of survival pathway activation

Primary human CD4+ T cells were re-stimulated using either 20 ng/ml phorbol 12-myristate 13-acetate (PMA; for ERK1/2 and AKT phosphorylation; Sigma) or 100 ng/ml IL6 (for STAT-3 phosphorylation; PeproTech) prior to flow cytometric analysis. MF cells and primary CD4+ T cells were fixed using CytofixTM buffer, then permeabilized using PhosflowTM Perm Buffer III (both BD Bioscience, San Jose, CA, USA), according to the manufacturer's instructions. After washing and resuspension, cells were incubated with phospho-flow antibodies (PE-CyTM7 Mouse anti-ERK1/2, pT202/pY204; PE Mouse anti-Akt, pS473; Alexa Fluor[®] 647 Mouse Anti-Stat3, pY705, all BD Bioscience) according to the manufacturer's instructions. Samples were analysed using the CytoFLEX flow cytometer and CytExpert software (Beckman Coulter, Indianapolis, IN, USA). Data analysis was performed using FlowJo v10 software (FlowJo, Ashland, OR, USA). Phosphorylation of signalling molecules in CD4+ T cells is reported as percent frequency, due to the heterogeneity of the CD4+ T cell population in primary cells isolated from PBMCs and because only a subset of T cells responds to T-cell receptor stimulus with robust

upregulation of phosphorylation of the evaluated signalling molecules. Phosphorylation of signalling molecules in CTCL cell lines, which have constitutively high levels of phosphorylated AKT, ERK1/2 and STAT-3, is reported as mean fluorescent intensity per cell.

Clinical MF samples

Skin biopsies of MF patients were collected at The University of Texas MD Anderson Cancer Center (Houston, TX, USA) between 2008 and 2010 under Institutional Review Board (IRB)-approved laboratory protocols 97-256, PA12-0267, PA12-0497, and PA15-0466. A single 20- μ m curl from 77 de-identified formalin-fixed paraffin-embedded (FFPE) samples and the associated de-identified pathology reports were transferred to miRagen under a biological material transfer agreement, which was reviewed by MD Anderson's IRB to ensure that patient confidentiality and consent were not compromised. Information regarding disease stage and lesion type was extracted from the pathology reports. RNA was extracted from the FFPE curls with the RecoverAllTM Total Nucleic Acid Isolation Kit for FFPE and quantitated by NanoDrop spectrophotometer (both ThermoFisher). Samples were analysed by qPCR for miR-155 quantitation at Covance Genomics Laboratories (Seattle and Redmond, WA, USA). Data analysis was performed at miRagen Therapeutics. Samples for which miR-155 was undetectable had no amplification of miR-155. Samples that were below the limit of quantitation had a miR-155 qPCR signal that was below the linear range of the assay. Normal skin FFPE samples from 10 individual donors were purchased from ILSBio (Chestertown, MD, USA), Proteogenex (Culver City, CA, USA) and AdeptBio (Memphis, TN, USA).

NanoString analysis

RNA extracted from MF and normal skin biopsies was profiled using a custom CodeSet (NanoString, Seattle, WA, USA). Raw NanoString Reporter Code Count (RCC) data files were analysed using the Bioconductor package for R (<https://www.bioconductor.org/>). Standard data normalization techniques were applied to the tissue sample gene expression data, using sets of negative and positive controls defined by NanoString as well as housekeeping genes, and were subjected to a presence/absence filter. Individual genes for which <80% of background subtracted samples were above 0 were excluded from further analysis. Fold-change in gene expression was calculated relative to the mean of three normal skin samples and then log₂ transformed.

Statistical tests

Differences in gene expression between groups were assessed with a Student's unpaired *t*-test. Comparisons of groups with

unequal variance were performed with a Mann-Whitney test. A *P*-value of 0.05 was used to determine significance in all tests unless otherwise noted.

Results

Cobomarsen is an optimized inhibitor of miR-155

In order to develop an optimized inhibitor of miR-155, we screened a panel of synthetic antimiR-155 oligonucleotides that had base-pairing complementarity to miR-155, and which were designed to competitively inhibit the interaction of miR-155 with its mRNA targets. The activity of these inhibitors was measured by the magnitude and significance of de-repression of four direct seed-matched targets of miR-155 [BACH1 (Skalsky *et al.*, 2007; O'Connell *et al.*, 2008; Yin *et al.*, 2008; Ceppi *et al.*, 2009), JARID2 (Escobar *et al.*, 2014; Norfo *et al.*, 2014), PICALM (O'Connell *et al.*, 2008) and INPP5D (also termed SHIP1; O'Connell *et al.*, 2009; Pedersen *et al.*, 2009; Yamanaka *et al.*, 2009)] in five CTCL lines. Note that the MF and HTLV-1+ CTCL cell lines (My-La, MJ, and HuT 102) and the unspecified cell line HH all expressed high levels of miR-155, whereas the SS cell line HuT 78 expressed a low level of miR-155 (Figure S1).

In response to treatment with each of the miR-155 inhibitors (Compounds A, B, C or cobomarsen), expression of the four direct targets significantly increased in the cell lines that overexpress miR-155 (*P* < 0.0001, Mann-Whitney test, Fig 1A and Figure S2), but not in the HuT 78 cell line that expresses a low level of miR-155 (Fig 1B). In magnitude of target engagement, cobomarsen was superior to the other antimiR-155 compounds in these cell lines.

Next, we assessed the dose-dependence and sequence-specificity of cobomarsen on miR-155 activity in MF and HTLV-1+ CTCL cell lines. In HuT 102 cells, the change in expression of the four seed-matched target genes increased with increasing dose of cobomarsen, and this change in expression was statistically significant at doses ≥ 1.0 μ mol/l (*P* < 0.0001, Mann-Whitney test, Fig 1C). In the My-La and MJ cell lines, changes in gene expression in response to cobomarsen were similarly dose-dependent (data not shown). In contrast, the change in gene expression with an unrelated control oligonucleotide was minimal and not dose-dependent (Fig 1C).

To compare cellular uptake of cobomarsen with the other inhibitors, unfacilitated delivery was compared with facilitated delivery (nucleofection) of cobomarsen and compound C in MJ cells. Following treatment of the cells with 10 μ mol/l of antimiR-155 inhibitors, the mean change in gene expression of three direct targets (BACH1, JARID2, PICALM) was calculated. Cobomarsen and compound C produced equivalent target de-repression when delivered via nucleofection, whereas cobomarsen showed greater target de-repression

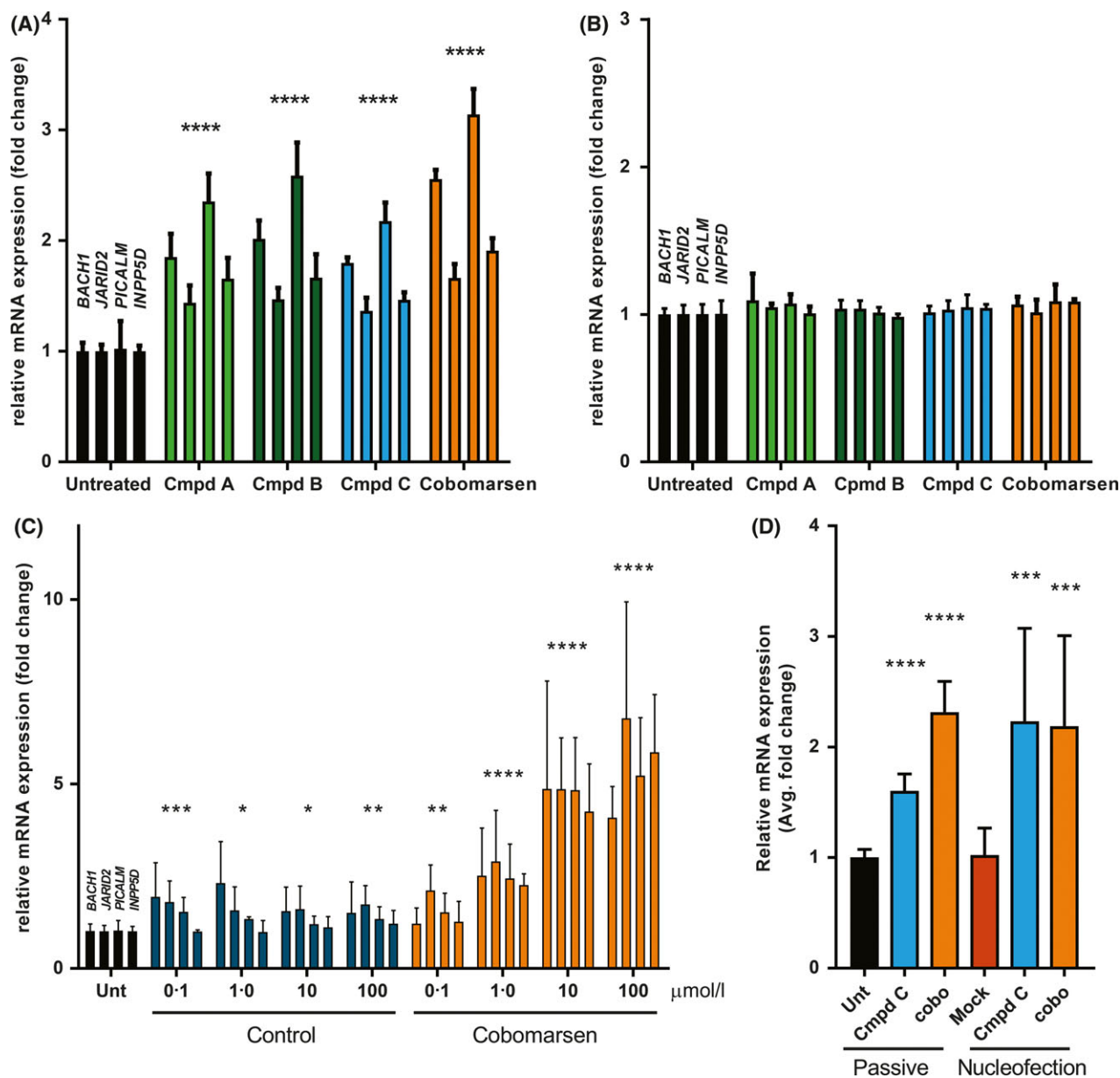


Fig 1. Identification of a miR-155 inhibitor optimized for functional uptake in cutaneous T-cell lymphoma (CTCL) cells. (A, B) Four inhibitors of miR-155 were evaluated in the HTLV-1+ CTCL cell line HuT 102 (A) and the Sezary cell line HuT 78 (B). Cells were incubated for 72 h in complete growth medium containing 10 μ mol/l of Compound A, B, C, or cobomarsen. Compounds were added directly to growth medium; no transfection agents were utilized. The activity of each antimiR-155 compound was evaluated by comparing the fold-change in expression by qRT-PCR of four direct targets of miR-155 relative to untreated cells. (C) Changes in expression of four direct targets of miR-155 in HuT 102 cells by cobomarsen treatment relative to untreated cells or treatment with a control oligonucleotide (control) were measured by qRT-PCR. (D) Comparison of passive uptake of cobomarsen with facilitated transfection (nucleofection) in MJ cells. Each bar represents the mean change in expression of target genes (*BACH1*, *JARID2*, *PICALM*) relative to untreated cells after the indicated treatment. Results are the mean of 3–11 replicates; error is standard deviation. * $P < 0.05$, ** $P < 0.01$, *** $P < 0.001$, or **** $P < 0.0001$ versus untreated cells by Mann–Whitney test for three or four genes. cmpd: compound; cobo: cobomarsen; Mock: indicates cells nucleofected without compound; Unt: untreated cells.

than compound C with passive uptake (Fig 1D). Furthermore, the magnitude of cobomarsen activity was equivalent when delivered passively or actively, demonstrating that this compound displays maximal uptake and activity with passive uptake. On the basis of these results in CTCL cell lines, cobomarsen was selected as the lead compound for further studies.

Cobomarsen inhibition of miR-155 reduces cellular proliferation and induces apoptosis in MF and HTLV-1+ CTCL cells

Overexpression of miR-155 has been reported to promote cellular proliferation and escape from apoptosis in malignant cells (Metzler *et al*, 2004; Eis *et al*, 2005; Costinean *et al*,

2006; O'Connell *et al*, 2008; Wang & Lee, 2009; Yamanaka *et al*, 2009; Babar *et al*, 2012; Kopp *et al*, 2013b; Gerloff *et al*, 2015; Moyal *et al*, 2017). To determine whether cobomarsen reverses these phenotypes by inhibiting miR-155 activity, we measured cellular proliferation and apoptosis in CTCL cells following treatment with cobomarsen. When HuT 102 cells were treated with cobomarsen, cellular proliferation decreased dramatically (Fig 2A), while apoptosis, as measured by caspase 3/7 activity, increased (Fig 2B). The control compound was tested in parallel with cobomarsen in

an independent experiment and did not affect either proliferation or apoptosis (Figure S3). The phenotypic impact of cobomarsen was compared to that of bexarotene, a retinoid that is approved in North America and Europe to treat CTCL. In HuT 102 cells, cobomarsen decreased cellular proliferation comparably to bexarotene, whereas cobomarsen had a greater impact on apoptosis induction than bexarotene (Fig 2A, B). In HuT 78 cells that do not express miR-155, cobomarsen had little effect on cellular proliferation or apoptosis (Fig 2C, D).

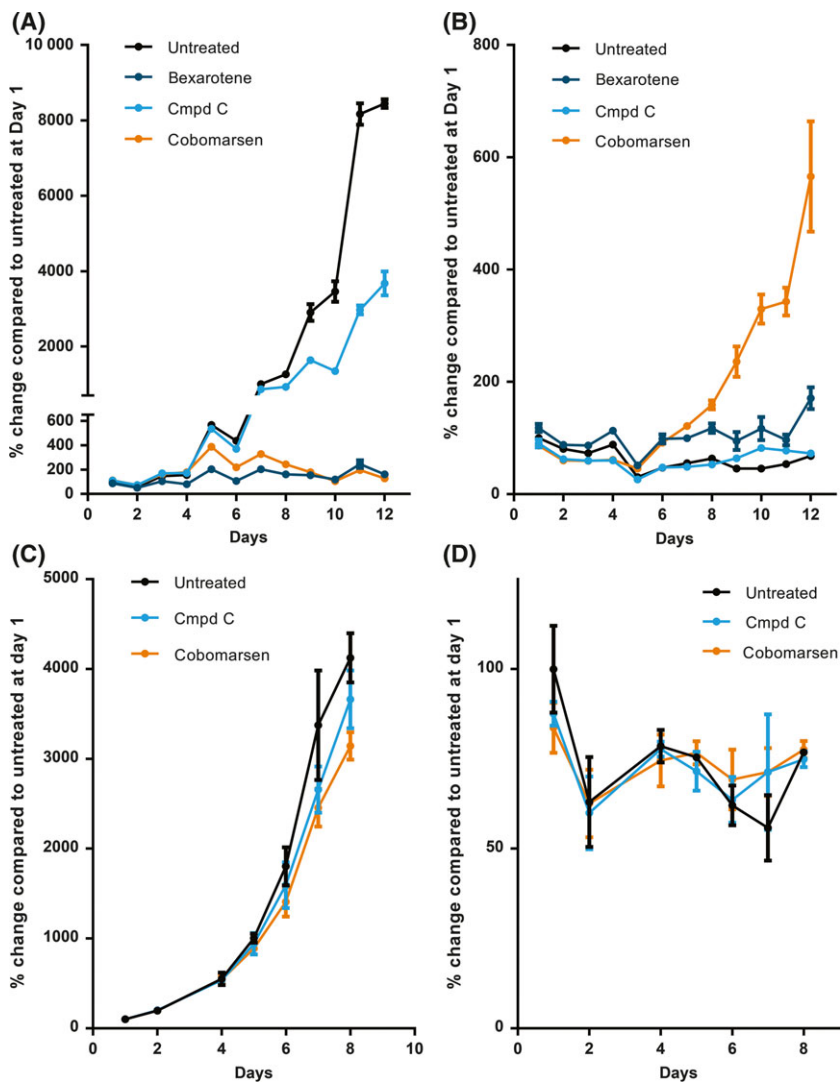


Fig 2. Cobomarsen reduces cellular proliferation and increases apoptosis in miR-155-overexpressing cells but not Sézary syndrome cells. (A, B) HuT 102 cells (high level of miR-155) were incubated in complete growth medium containing 10 μ mol/l cobomarsen, Compound C (Cmpd C), or bexarotene for 12 days. (A) Percent change in cellular adenosine triphosphate (ATP) levels, which correlates linearly with total cell number, relative to the untreated cells harvested at Day 1. (B) Percent change in caspase 3/7 activity, a surrogate measure of apoptosis, relative to untreated cells harvested at Day 1. Because proliferating cells have basal caspase 3/7 activity, the caspase 3/7 activity was normalized to cellular ATP levels. (C, D) HuT 78 cells (low level of miR-155) were treated with 10 μ mol/l cobomarsen for 8 days. Panels C and D show the percent change in cellular ATP and caspase 3/7 activity, respectively, as described for Panels A and B. The HuT 102 results are the mean of four replicates with the exception of one timepoint collected for the caspase assay (3 replicates); error is standard error. The HuT 78 results are the mean of three replicates; error is standard deviation.

Identification of a gene expression signature of cobomarsen in MF and HTLV-1+ CTCL cell lines demonstrating target engagement and mechanism of action

Although microRNAs can regulate hundreds to thousands of targets, the biological pathways regulated by microRNAs are not always obvious from an examination of their direct targets (Linsley *et al*, 2007). To gain a more complete understanding of the mechanism of action of cobomarsen in CTCL cell lines, whole transcriptome profiling was performed on three MF or HTLV-1+ CTCL cell lines (My-La, HuT 102, MJ) and the SS cell line (HuT 78). Cells were treated with cobomarsen for 4 or 8 days to identify direct or downstream targets of miR-155, respectively. We hypothesized that downstream gene signatures might be informative of the pathways and networks impacted by cobomarsen in this cell type, an approach that has elucidated the mechanisms of action of other microRNAs (Linsley *et al*, 2007). Unique sets of genes were identified that were regulated at the early time point (Day 4) or the late time point (Day 8), as well as some genes that were regulated at both time points (Fig 3A shows representative results in the HuT 102 cell line). We analysed the gene signature from each time point for regulation of seed-matched targets and calculated the enrichment for target regulation by hypergeometric p-value (Fig 3B). Following exposure to cobomarsen, each cell line signature was significantly enriched for miR-155 seed-matched targets ($P < 1 \times 10^{-36}$, Fig 3B), confirming on-target activity for cobomarsen. Notably, the signatures include the miR-155 seed-matched targets *BACH1*, *PICALM* and *JARID2* that we confirmed are regulated by cobomarsen in MF and HTLV-1+ CTCL cells (Fig 1A and Figure S2). A subset of the genes regulated by cobomarsen at Day 4 was selected for confirmatory analysis by qRT-PCR. All the genes examined were confirmed to be de-repressed by cobomarsen, whereas no target regulation resulted from treatment with a control oligonucleotide (Figure S4). No significant functional annotation was observed at Day 4 (analysis not shown).

Transcriptome profiling following 8 days of exposure to cobomarsen in the three cell lines with elevated miR-155 expression revealed statistically significant regulation of 3770 genes in HuT 102 cells, 3522 genes in MJ cells and 2963 genes in My-La cells. Notably, few genes ($n = 159$) were significantly regulated at Day 8 in the SS cell line HuT 78 with low expression of miR-155. Functional analysis of each cell line gene signature using DAVID analysis as well as GO terms determined that all three cell lines were enriched for cell cycle and apoptosis (Fig 3B).

Examination of the gene expression profiles revealed a set of genes regulated similarly in all three cell lines, as well as genes that were regulated uniquely in each cell line. In order to derive a set of genes to serve as translational pharmacodynamic biomarkers for clinical assessment of cobomarsen, a set of genes regulated in common in all three MF or

HTLV-1+ CTCL cell lines was identified. We reasoned that requiring consistent regulation in these biologically diverse cell lines would yield a biomarker signature that would be more robust to biological (clinical) diversity. We identified a gene signature for each time point (Day 4 and Day 8) that was significantly up-regulated in all three cell lines or significantly down-regulated in all three cell lines with no filter on the magnitude of gene expression. The two gene signatures were then combined into a single gene list of cobomarsen pharmacodynamic biomarkers, which we will refer to as the common signature. Therefore, the common signature contains genes that are regulated only at Day 4, only at Day 8 or at both time points. The common signature contains 587 genes comprising early (direct) targets and downstream (indirect) targets regulated by cobomarsen (Fig 3C). This common signature includes the direct targets *BACH1*, *PICALM* and *JARID2* (Fig 1A–C and Figure S2); *INPP5D* is not on the gene list because it was significantly regulated in only two of the three cell lines. Analysis of the common gene signature using the DAVID bioinformatics resource demonstrated enrichment for functional terms including mitotic cell cycle and response to DNA damage stimulus. Analysis of the common gene signature using ingenuity pathway analysis (IPA) software demonstrated that this set of genes is enriched for survival pathways including HGF/c-MET, PI3K/AKT and JAK/STAT, as well as cytokine signalling (IL17, IL3, granulocyte-macrophage colony-stimulating factor [GM-CSF]) (Table SI). Notably, none of these cobomarsen pharmacodynamic biomarker genes were regulated in the HuT 78 cell line, which does not overexpress miR-155 (Fig 3C).

Cobomarsen inhibits signalling through the JAK/STAT, PI3K/AKT, and MAPK pathways

Because direct targets of miR-155 include genes that negatively regulate signalling through the PI3K/AKT, JAK/STAT and MAPK signalling pathways (O'Connell *et al*, 2009; Viernes *et al*, 2014; Yang *et al*, 2015a,b), we hypothesized that inhibition of miR-155 would reduce signalling through all three pathways simultaneously. To test our hypothesis, we stimulated primary human CD4+ T cells through the T-cell receptor for 2 days and then treated the cells with cobomarsen or idelalisib (PI3K inhibitor), U0126 (MAPK inhibitor) or ruxolitinib (JAK inhibitor). Cobomarsen reduced signalling through all three pathways, as measured by reduced phosphorylation of the downstream signalling proteins AKT, ERK1/2, and STAT-3 (Fig 4A). Inhibition of ERK1/2 and AKT phosphorylation with 10 μ mol/l cobomarsen was similar to that observed with the respective kinase inhibitors, while inhibition of STAT-3 phosphorylation by 50 μ mol/l cobomarsen was comparable to ruxolitinib. When the MF cell line My-La was similarly treated with cobomarsen or the pathway-specific inhibitors, cobomarsen again reduced signalling through all three survival

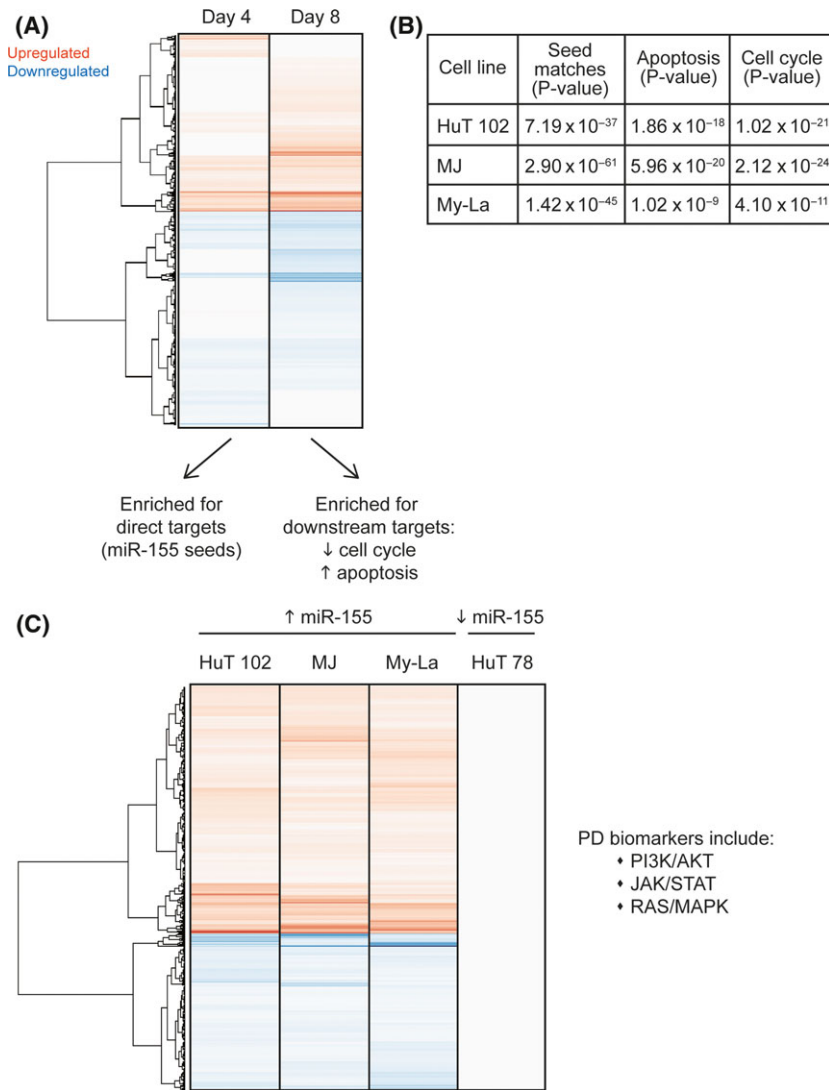


Fig 3. Cobomarsen regulates genes associated with cell cycle and apoptosis in mycosis fungoides (MF) and human lymphotropic virus type 1 (HTLV-1+) cutaneous T-cell lymphoma (CTCL) cell lines. (A) Genes differentially regulated by cobomarsen in HuT 102 cells following 4 or 8 days of exposure. Red = genes upregulated by cobomarsen compared with untreated cells, blue = genes down-regulated by cobomarsen compared with untreated cells (Benjamini–Hochberg false discovery rate $P < 0.05$). (B) Enrichment for seed matches or functional annotation in genes significantly regulated by cobomarsen in CTCL cell lines. Enrichment was calculated by hypergeometric P -value for the overlap with miR-155 seed-matched targets or with genes associated with specific GO terms. (C) Identification of a common signature of genes in the three MF or HTLV-1+ CTCL cell lines with high miR-155 expression following 8 days of exposure to cobomarsen; genes were either up-regulated in all three cell lines or down-regulated in all three cell lines. None of the genes were significantly regulated in the HuT 78 cell line with low expression of miR-155.

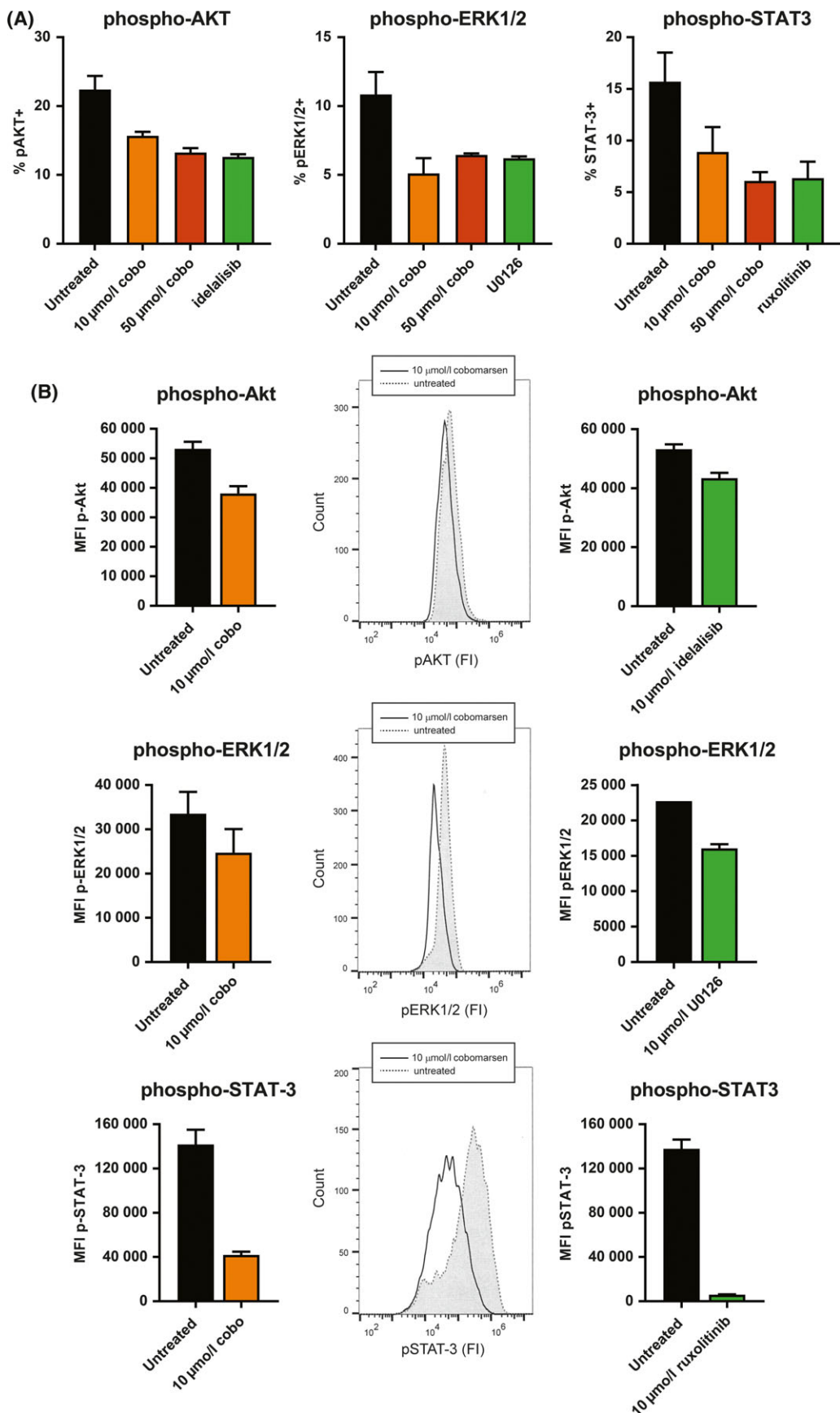
pathways to an extent similar to each small molecule inhibitor (Fig 4B, C).

miR-155 is upregulated in MF clinical specimens and correlates with lesion type

We measured miR-155 expression by qRT-PCR in RNA isolated from 77 MF and 10 normal skin biopsy samples. FFPE MF samples were collected at MD Anderson Cancer Center between 2008 and 2010. Of the 77 MF biopsy samples, 57 had quantifiable miR-155, 17 had miR-155 values below the limit of quantitation and three had undetectable miR-155. Of the 10 normal skin samples, 3 samples had quantifiable miR-155, and the remaining 7 samples had miR-155 values below the limit of quantitation. There was no apparent correlation between miR-155 expression and CTCL disease stage (Fig 5A), but miR-155 expression increased with increasing lesion severity (patch to plaque to tumour) (Fig 5B).

Expression of cobomarsen pharmacodynamic biomarker genes correlates with miR-155 expression and lesion type in MF clinical samples

To determine whether the pharmacodynamic biomarkers we identified for cobomarsen in MF and HTLV-1+ CTCL cell lines are dysregulated in the clinical context of MF, we examined the expression of these biomarker genes in FFPE skin biopsies from MF patients. Using a custom NanoString CodeSet consisting of the previously described common gene signature (Fig 3C) as well as a set of eleven disease-associated genes, we compared gene expression in 22 MF biopsies with quantifiable miR-155 expression to three normal skin biopsies. The MF biopsies were selected to represent all lesion types, all stages of disease, and a range of miR-155 expression. We found that expression of the pharmacodynamic biomarkers segregated the MF biopsies into two main clusters: the first cluster with high levels of miR-155 consisted predominantly of tumour lesions, while the second cluster



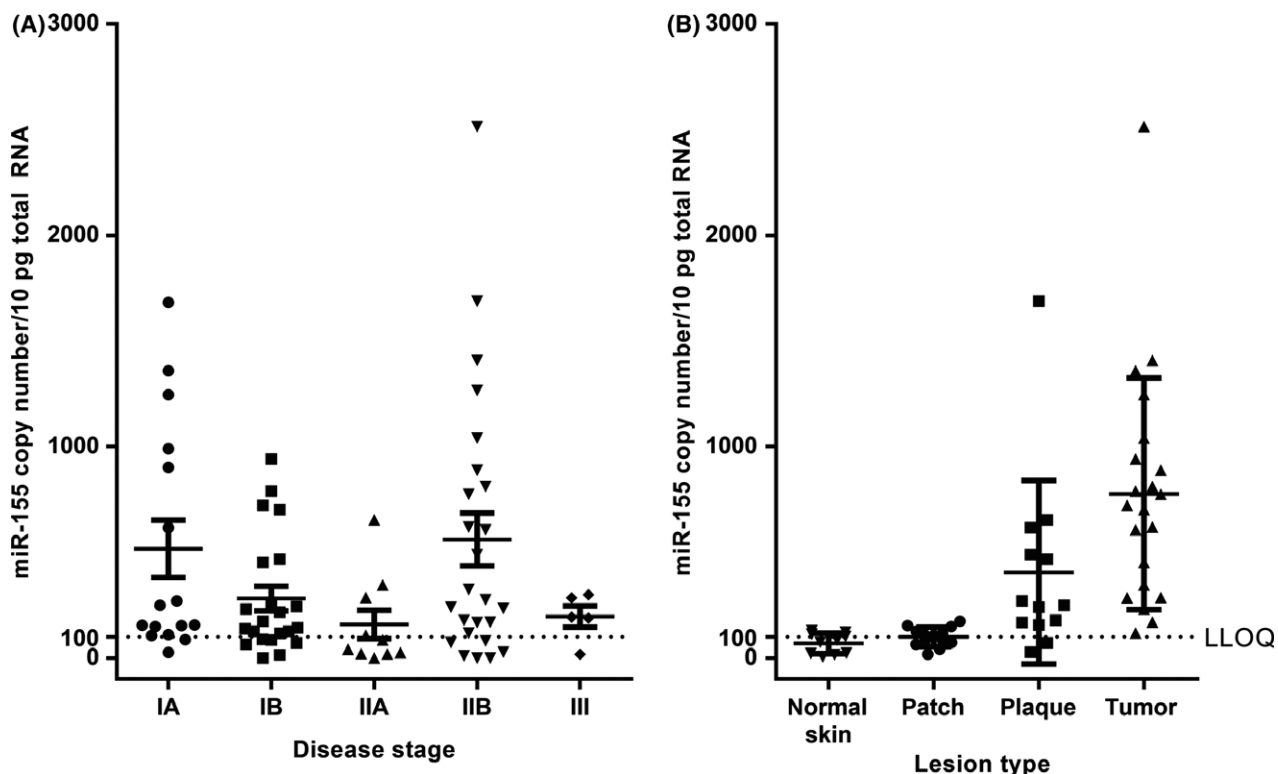


Fig 5. Clinical specimens showed that miR-155 expression is dependent on lesion type but not disease stage. miR-155 copy number measured by qRT-PCR of 57 mycosis fungoides lesions and 10 biopsies of normal skin from healthy donors. (A) Expression of miR-155 in samples classified by disease stage at the time of biopsy collection. (B) Expression of miR-155 in samples classified by lesion type, as noted in pathology reports. miR-155 copy number in each sample is indicated by the dots, mean copy number by the long horizontal line, and standard error by the vertical line. LLOQ, lower limit of quantification.

with low-to-intermediate levels of miR-155 consisted predominantly of patch and plaque lesions (Fig 6A). The biopsies in the first cluster (tumour lesions) also had high levels of CD3, a T-cell marker, whereas the biopsies in the second cluster (patch and plaque lesions) had low to intermediate levels of CD3. Annotation analysis of genes down-regulated in MF biopsies compared to normal skin (most down-regulated in tumours, then plaques, then patches) showed enrichment of seed matches (octamer or heptamer seed match $P < 0.01$, data not shown), suggesting that direct targets of miR-155 are repressed as miR-155 level increases. Conversely, the set of genes up-regulated in MF biopsies compared to normal skin (most up-regulated in tumours, then plaques, then patches) was not enriched for seed matches. IPA

analysis of these up-regulated genes showed increased activation of the T cell helper type 1 (Th1) and Th2 pathways, consistent with the T cell activation associated with MF. This set of genes also demonstrated increased regulation of the HGF/

c-MET, JAK/STAT, ERK/MAPK and PI3K/AKT survival signalling pathways and the GM-CSF, IL-17, and IL-3 cytokine signalling pathways, and reduced G1/S cell cycle checkpoint regulation (Table SII). These genes are likely to be downstream (indirect) targets, indicative of the role of elevated miR-155 in promoting cellular proliferation, survival, inflammation, and genome instability.

We wanted to perform a more direct comparison of cobomarsen pharmacodynamic biomarker expression in MF

Fig 4. Cobomarsen simultaneously inhibits signalling through the JAK/STAT, PI3K/AKT and MAPK pathways in primary human activated T cells or MF cell lines. (A) Human CD4+ T cells were isolated, stimulated for 2 days with anti-CD3/anti-CD28-coated Dynabeads in the presence of IL2, followed by re-stimulation with either PMA (for ERK1/2 and AKT phosphorylation) or with IL6 (for STAT-3 phosphorylation), and cultured with 10 or 50 μ mol/l cobomarsen (cobo) or the indicated inhibitors of AKT (idelalisib), ERK1/2 (U0126) or STAT-3 (ruxolitinib). (B) My-La cells were treated for 7 days with cobomarsen (10 μ mol/l), for 7 days with AKT inhibitor (idelalisib, 10 μ mol/l), for 4 h with the ERK inhibitor (U0126, 10 μ mol/l) or for 4 days with the STAT inhibitor (ruxolitinib, 10 μ mol/l). Cells were stained and quantitated by flow cytometry for phosphorylated AKT, ERK1/2 or STAT-3. Where error is shown, the results are the mean of two replicates; error is standard deviation. FI, fluorescence intensity; MFI, mean FI.

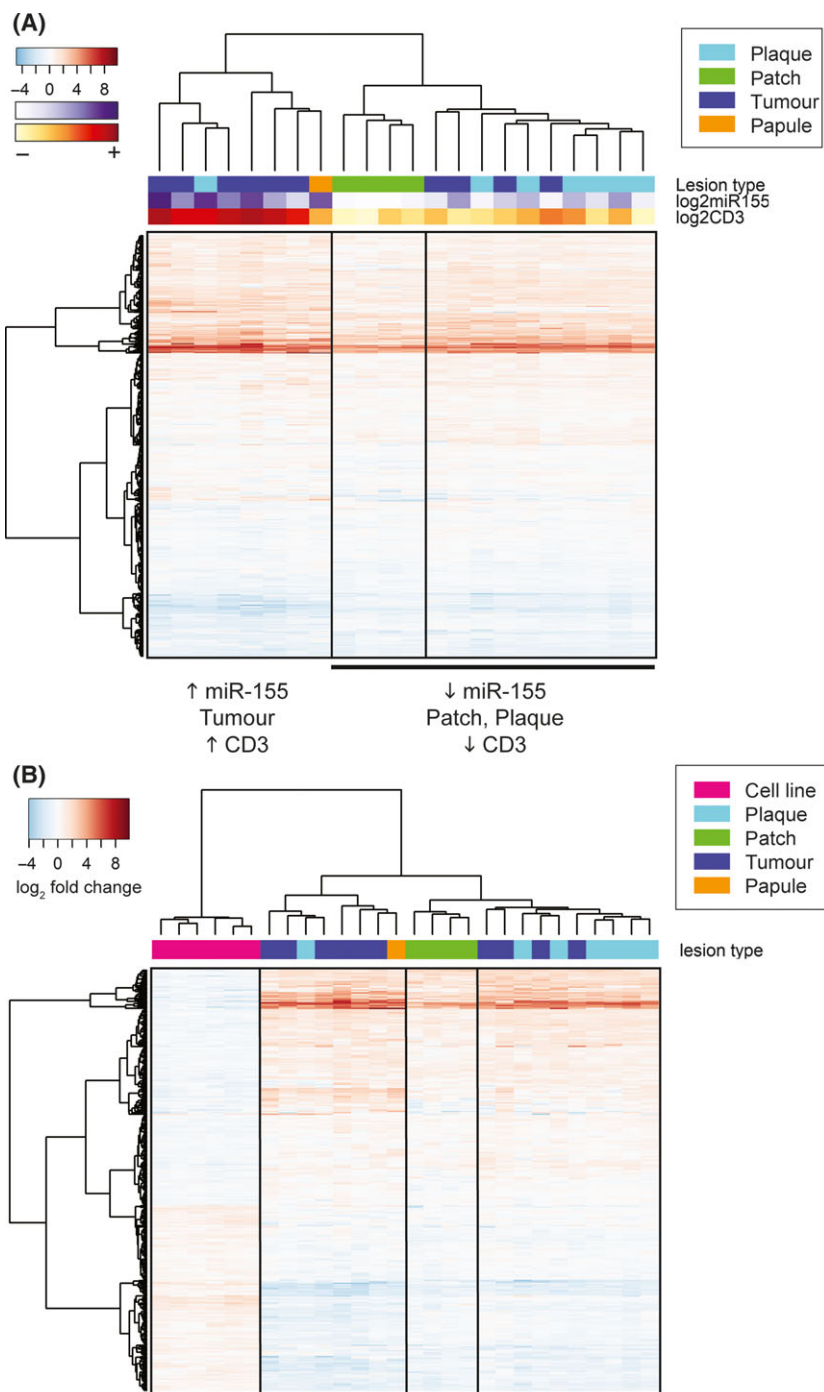


Fig 6. Cobomarsen pharmacodynamic biomarkers differentiate mycosis fungoides (MF) lesions according to lesion type. Twenty-two MF biopsies were analysed for expression of the cobomarsen common gene signature in MF or HTLV-1+ cutaneous T-cell lymphoma (CTCL) cell lines. Biopsies represented all lesion types, stages of disease, and a range of miR-155 expression from approximately 100–2500 copies/10 pg total RNA. (A) Hierarchical cluster of pharmacodynamic biomarker genes differentially expressed in MF biopsies compared to normal skin. Red = increased gene expression in MF biopsies, blue = decreased gene expression in MF biopsies. Overlaid on the hierarchical cluster are the lesion type (patch, plaque, papule, tumour), the \log_2 expression of miR-155 on a scale of low expression (white) to high expression (purple), and \log_2 expression of CD3 on a scale of low expression (yellow) to high expression (red). (B) Hierarchical cluster of 299 genes showing reciprocal regulation in MF biopsies compared to cobomarsen-treated CTCL cell lines. Shown is the differential expression for cobomarsen treatment *versus* saline treatment for the three CTCL cell lines at two time points (4 and 8 days) of cobomarsen exposure, and the differential expression for the 22 MF biopsies *versus* normal skin. Overlaid on the hierarchical cluster is the identification of the sample type (cell line, patch, plaque, papule, tumour).

clinical biopsies with expression in cobomarsen-treated cell lines. We calculated \log_2 fold-change in gene expression of the biomarkers for MF clinical biopsies compared to normal skin, and for cobomarsen-treated compared to untreated MF or HTLV-1+ CTCL cell lines, then used hierarchical clustering to visualize the change in expression of all biomarker genes across all samples. We found that some genes were reciprocally expressed between MF biopsies and cobomarsen-treated cell lines, while other genes were expressed similarly

across all samples (Fig 6B). The subset of genes with similarity of expression across all samples was not enriched for any functional annotation. The subset of genes with reciprocal expression was enriched for survival signalling, cell cycle checkpoint regulation and cytokine signalling (Fig 6B, Table I). Interestingly, IPA analysis of these genes demonstrated that T cell activation, survival signalling pathways, and cytokine signalling pathways were up-regulated and activated in MF clinical biopsies but down-regulated and

inactivated in cobomarsen-treated cell lines, whereas checkpoint regulation was down-regulated and inactivated in MF biopsies but up-regulated and activated in cobomarsen-treated MF or HTLV-1+ CTCL cell lines (Table I).

Discussion

Because miR-155 has been implicated in the pathogenesis of MF, several groups have hypothesized that miR-155 might be a potential therapeutic target in MF (Kopp *et al*, 2013a; Moyal *et al*, 2017). In this study, we developed cobomarsen, a synthetic locked nucleic acid-modified oligonucleotide inhibitor of miR-155. Oligonucleotides have been proven to be viable antisense therapies for several drug targets (Janssen *et al*, 2013; Polychronopoulos & Tziomalos, 2017). Cobomarsen, which has base-pairing complementarity to miR-155, was chosen from a panel of miR-155 inhibitors for its superiority in de-repression of miR-155 direct targets (Fig 1A, B and Figure S2) and unfacilitated uptake (Fig 1D). We demonstrated that cobomarsen activity was specific to miR-155 inhibition, as shown by the differential effects of cobomarsen on CTCL cells with high *versus* low expression of miR-155 (Figs 1A, B, 2 and 3C and Figure S2) and by its effects on seed-matched targets (Fig 3B). We also showed the dose-dependence (Fig 1C) and sequence-specificity (Fig 1C and Figures S3 and S4) of cobomarsen in CTCL cell lines.

We demonstrated that cobomarsen inhibits cell proliferation and induces apoptosis in MF and HTLV-1+ CTCL cells (Fig 2 and Figure S3), which was confirmed in transcriptome analysis (Fig 3B). In its ability to inhibit cell proliferation, cobomarsen was comparable to bexarotene (Fig 2A), one of the most commonly prescribed systemic treatments for MF. However, bexarotene did not induce apoptosis (as measured by the activity of the caspase 3/7 proteins) in the HuT 102 cell line, whereas cobomarsen did (Fig 2B). These results differ from those of Zhang *et al* (2002), in which bexarotene was shown to induce apoptosis (as measured by Annexin V cell staining and caspase 3 activation) in MJ, HuT 78, and HH cell lines. Both studies used the same concentration of bexarotene (10 μ mol/l), so the results may differ due to variations in the cell lines, experimental conditions or bexarotene sourcing.

In order to understand the molecular mechanism of cobomarsen in CTCL cells, we leveraged global expression analysis to determine the impact of cobomarsen on gene pathways and networks. Gene expression changes in CTCL have been studied extensively (Dulmage & Geskin, 2013; Litvinov *et al*, 2017) and multiple studies have identified targets for miR-155 (Loeb *et al*, 2012; Neilsen *et al*, 2013; Xie *et al*, 2014). To our knowledge, this is the first report of a transcriptome analysis of miR-155-regulated targets in MF and HTLV-1+ CTCL. We identified a gene signature for cobomarsen comprising 587 direct and downstream targets of cobomarsen that were regulated in all three MF and HTLV-1+ CTCL cell lines. We demonstrated that these pharmacodynamic biomarkers of cobomarsen are specific for miR-155 inhibition, as

demonstrated by their differential expression in CTCL cell lines with high *versus* low expression of miR-155 (Fig 3C).

The gene signature we identified is associated with the cell cycle and apoptosis (Fig 3B), which is consistent with the effects of cobomarsen on these cells (Fig 2). In particular, the gene signature is enriched for survival signalling pathways including HGF/cMet, PI3K/AKT, JAK/STAT and p38 MAPK (Table SI). We demonstrated that cobomarsen reduced signalling in these parallel survival pathways in both stimulated T cells and MF cells, comparable to the effects of specific inhibitors of each pathway (Fig 4). These data support our proposed mechanism of action of cobomarsen: disruption of the constitutive survival loop in activated or transformed T cells by disrupting multiple pro-survival pathways simultaneously. These findings expand upon studies demonstrating a role for miR-155 in regulation of the PI3K/AKT pathway (Huang *et al*, 2012) and the JAK/STAT pathway (Kopp *et al*, 2013a; Rasmussen *et al*, 2015).

One limitation of the cell line experiments is the question of whether these transformed patient-derived cell lines reflect MF (Netchiporuk *et al*, 2017). Our transcriptome profiles of the three cell lines revealed that some genes were regulated uniquely in each cell line. The cell line-specific signatures might reflect individual patient variability, different stages of disease, or the different origins of each cell line (HuT 102 was derived from lymph node (Poiesz *et al*, 1980), MJ was derived from peripheral blood and My-La was derived from a skin lesion). Additionally, it has been suggested that the HuT 102 and MJ cell lines are more representative of adult T-cell lymphocytic leukaemia (ATLL) due to the presence of HTLV-1 (Netchiporuk *et al*, 2017). Therefore, it was important to compare the findings for miR-155 expression and biomarker gene expression in the cell lines to clinical MF biopsies.

To determine whether the gene signature we identified from CTCL cell lines translated to clinical samples, we examined miR-155 and biomarker gene expression in FFPE MF biopsy samples. We found that miR-155 expression was increased in 57 of the 77 MF samples studied, consistent with one published report (Maj *et al*, 2012). We found increasing miR-155 expression in biopsy samples with increasing severity of lesion type (patch to plaque to tumour) (Figs 5B and 6A), consistent with reports demonstrating increased expression of miR-155 in tumour-stage MF (van Kester *et al*, 2011; Moyal *et al*, 2013; Sandoval *et al*, 2015; Garaicoa *et al*, 2016). The differential expression of the pharmacodynamic biomarker genes was sufficient to cluster biopsies according to lesion type (patch, plaque, or tumour) (Fig 6A). These clusters also reflected differential expression of miR-155 and CD3, a T-cell marker, which suggests that expression of the pharmacodynamic biomarkers and miR-155 reflects the density of T cells in the lesion. Note, however, that both malignant and non-malignant reactive T cells have been detected in MF skin biopsies, and miR-155 has been expressed in both types of T cells (Kopp *et al*, 2013b; Moyal *et al*, 2013).

Table I. Functional annotation enrichment for genes showing reciprocal expression and regulation in clinical mycosis fungoides (MF) biopsies compared to cutaneous T-cell lymphoma (CTCL) cell lines treated with cobomarsen. Shown are the canonical pathways enriched ($P < 0.05$, $-\log(P\text{-value}) \geq 1.3$) for the genes identified as having reciprocal gene regulation in clinical MF biopsies *versus* MF and human lymphotropic virus type 1 positive (HTLV-1+) CTCL cell lines exposed to cobomarsen. The predicted activation state is based on the z-score as determined by IPA analysis.

Ingenuity canonical pathways	−log (<i>P</i> -value)	Predicted activation state		
		Cobomarsen in cell lines	MF biopsies	Genes
HGF signalling	3.25	Inactive	Active	PRKCI, RRAS2, MAPK1, IL6, PTGS2, STAT3, MAP2K1, CDK2
PI3K/AKT signalling	3.06	Inactive	Active	RRAS2, MAPK1, FOXO3, TSC2, YWHAZ, PTGS2, MAP2K1, EIF4EBP1
NRF2-mediated oxidative stress response	2.98	Inactive	Active	PRKCI, RRAS2, MAPK1, DNAJC19, UBE2K, DNAJB1, NFE2L2, MAP2K1, CLPP, BACH1
IGF-1 signalling	2.78	Inactive	Active	PRKCI, RRAS2, MAPK1, FOXO3, YWHAZ, STAT3, MAP2K1
Oncostatin M signalling	2.66	Inactive	Active	RRAS2, MAPK1, STAT3, MAP2K1
Thrombopoietin signalling	2.38	Inactive	Active	PRKCI, RRAS2, MAPK1, STAT3, MAP2K1
mTOR signalling	2.35	Inactive	Active	PRKCI, RRAS2, MAPK1, DDIT4, TSC2, EIF3J, FKBP1A, RPS6KCI, EIF4EBP1
Insulin receptor signalling	2.16	Inactive	Active	PRKCI, RRAS2, MAPK1, FOXO3, TSC2, MAP2K1, EIF4EBP1
STAT3 pathway	2.14	Inactive	Active	RRAS2, MAPK1, STAT3, IGF2R, MAP2K1
Cell cycle: G2/M DNA damage checkpoint regulation	2.08	Active	Inactive	TOP2B, WEE1, YWHAZ, BORA
CD40 signalling	2.05	Inactive	Active	MAPK1, PTGS2, STAT3, MAP2K1, TRAF1
JAK/Stat signalling	1.94	Inactive	Active	RRAS2, MAPK1, IL6, STAT3, MAP2K1
IL-3 signalling	1.94	Inactive	Active	PRKCI, RRAS2, MAPK1, STAT3, MAP2K1
FLT3 signalling in haematopoietic progenitor cells	1.94	Inactive	Active	RRAS2, MAPK1, STAT3, MAP2K1, EIF4EBP1
Prolactin signalling	1.94	Inactive	Active	PRKCI, RRAS2, MAPK1, STAT3, MAP2K1
α-Adrenergic signalling	1.9	Inactive	Active	CALM1 (includes others), PRKCI, RRAS2, MAPK1, MAP2K1
ERK/MAPK signalling	1.82	Active	Inactive	PRKCI, H3F3A/H3F3B, RRAS2, MAPK1, YWHAZ, STAT3, MAP2K1, EIF4EBP1
CNTF signalling	1.81	Inactive	Active	RRAS2, MAPK1, STAT3, MAP2K1
Acute myeloid leukaemia signalling	1.8	Inactive	Active	RRAS2, MAPK1, STAT3, MAP2K1, EIF4EBP1
PI3K signalling in B lymphocytes	1.76	Inactive	Active	CALM1 (includes others), PRKCI, RRAS2, MAPK1, FOXO3, MAP2K1
ERK5 signalling	1.71	Inactive	Active	RRAS2, FOXO3, YWHAZ, RPS6KCI
Endometrial cancer signalling	1.69	Inactive	Active	RRAS2, MAPK1, FOXO3, MAP2K1
Cholecystokinin/Gastrin-mediated signalling	1.64	Inactive	Active	PRKCI, RRAS2, MAPK1, PTGS2, MAP2K1
Role of NFAT in regulation of the immune response	1.62	Inactive	Active	CALM1 (includes others), RRAS2, CSNK1G1, CD80, MAPK1, CSNK1A1, MAP2K1
ErbB2-ErbB3 signalling	1.6	Inactive	Active	RRAS2, MAPK1, STAT3, MAP2K1
Chemokine signalling	1.6	Inactive	Active	CALM1 (includes others), RRAS2, MAPK1, MAP2K1
Mouse embryonic stem cell pluripotency	1.57	Inactive	Active	RRAS2, MAPK1, SMAD5, STAT3, MAP2K1
GM-CSF signalling	1.52	Inactive	Active	RRAS2, MAPK1, STAT3, MAP2K1
Sirtuin signalling pathway	1.45	Inactive	Active	PPID, H3F3A/H3F3B, MAPK1, TIMM9, FOXO3, NAMPT, STAT3, NFE2L2, POLR3D
Non-small cell lung cancer signalling	1.43	Inactive	Active	RRAS2, MAPK1, FOXO3, MAP2K1
IL-17A signalling in airway cells	1.41	Inactive	Active	MAPK1, IL6, STAT3, MAP2K1
Cyclins and cell cycle regulation	1.4	Inactive	Active	CDKN2D, CCNH, WEE1, CDK2
PTEN signalling	1.36	Inactive	Active	RRAS2, MAPK1, FOXO3, IGF2R, MAP2K1
Role of NANOG in mammalian embryonic stem cell pluripotency	1.34	Inactive	Active	RRAS2, MAPK1, SMAD5, STAT3, MAP2K1
Synaptic long term potentiation	1.34	Inactive	Active	CALM1 (includes others), PRKCI, RRAS2, MAPK1, MAP2K1
Pancreatic adenocarcinoma signalling	1.33	Inactive	Active	MAPK1, PTGS2, STAT3, MAP2K1, CDK2
fMLP signalling in neutrophils	1.3	Inactive	Active	CALM1 (includes others), PRKCI, RRAS2, MAPK1, MAP2K1

We compared our biomarker gene signature to published results comparing gene signatures for MF *versus* normal skin (Shin *et al*, 2007; Litvinov *et al*, 2010, 2015; van Kester *et al*, 2012). While the overlap in gene signatures across these studies was variable, pathway analysis showed similarities in enrichment for immune response, T cell activation, mitosis, cell cycle and cell division, consistent with the T cell origin of MF and the proliferative phenotype of the malignant cells. These results highlight the consistency of the molecular biology underlying MF pathology across different patient subsets and analysis methods and confirm the relevance of the cobomarsen-dependent signature for MF.

Collectively, these data demonstrate that the set of pharmacodynamic biomarker genes identified for cobomarsen in MF cell lines is dysregulated in the clinical setting of MF lesions. This set of biomarkers represents genes involved in cellular proliferation and survival, T cell activation and cytokine signalling and genomic stability. The observation that expression of these biomarkers corresponds to miR-155 expression level, lesion type and T cell density in clinical biopsies reinforces the conclusion that the pathology of disease progression in MF is associated with increased expression of miR-155, increased density of malignant or activated T cells, and dysregulation of multiple biological pathways.

Intriguingly, pharmacodynamic gene signatures that were up-regulated and activated in clinical MF biopsies, including those associated with T cell activation and survival signalling, were down-regulated and inactivated in MF and HTLV-1+ CTCL cells treated with cobomarsen, whereas genes associated with checkpoint regulation that were down-regulated and inactivated in MF biopsies were up-regulated and activated in response to cobomarsen in cell lines (Fig 6B, Table I). These data suggest that multiple biological pathways dysregulated and associated with the pathology of MF are associated with increased miR-155 expression and can be reversed by inhibition of miR-155 activity. Therefore, a microRNA-based therapy, such as cobomarsen might restore homeostasis to multiple dysregulated gene pathways and networks in MF.

Cobomarsen is currently being evaluated in a phase 1 study of patients with certain lymphomas and leukaemias, including CTCL, MF subtype, and ATLL, to characterize the safety, tolerability and pharmacokinetics of this miR-155 inhibitor (NCT02580552). The gene signature identified in this study will be used as a translational pharmacodynamic biomarker for cobomarsen in the phase 1 study.

References

Babar, I.A., Czochor, J., Steinmetz, A., Weidhaas, J.B., Glazer, P.M. & Slack, F.J. (2011) Inhibition of hypoxia-induced miR-155 radiosensitizes hypoxic lung cancer cells. *Cancer Biology & Therapy*, **12**, 908–914.

Babar, I., Cheng, C., Booth, C., Liang, X., Weidhaas, J., Saltzman, W. & Slack, F. (2012) Nanoparticle-based therapy in an in vivo micro-RNA-155 (miR-155)-dependent mouse model of lymphoma. *Proceedings of the National Academy of Sciences of the United States of America*, **109**, e1695–e1704.

Ballabio, E., Mitchell, T., van Kester, M.S., Taylor, S., Dunlop, H.M., Chi, J., Tosi, I., Vermeer, M.H., Tramonti, D., Saunders, N.J., Boultonwood, J., Wainscoat, J.S., Pezzella, F., Whittaker, S.J., Tensen, C.P., Hatton, C.S. & Lawrie, C.H. (2010) MicroRNA expression in Sezary syndrome: identification, function, and diagnostic potential. *Blood*, **116**, 1105–1113.

Bartel, D.P. (2009) MicroRNAs: target recognition and regulatory functions. *Cell*, **136**, 215–233.

Ceppi, M., Pereira, P., Dunand-Sauthier, I., Baras, E., Reith, W., Santos, M. & Pierre, P. (2009) MicroRNA-155 modulates the

Acknowledgements

This work was funded by miRagen Therapeutics, Inc., Boulder, CO, USA, which has filed worldwide patent applications directed to cobomarsen. We thank the miRagen chemistry group for design and synthesis of the oligonucleotide inhibitors and Brent Dickinson and Kristin Schroeder for technical assistance. Editorial assistance was provided by Helen Kim, MD, and funded by miRagen Therapeutics.

Competing interests

A.L.J., M.H., J.M.L. and X.B. are employed by, and own stock in miRagen Therapeutics. A.G.S. was employed by miRagen Therapeutics when the study was conducted and owns stock in miRagen. M.D. is a consultant to miRagen Therapeutics. M.T. discloses no competing interests.

Author contributions

A.L.J., A.G.S. and M.H. designed the research studies. M.H. and X.B. performed the research. A.L.J., A.G.S., M.H. and X.B. performed data analysis. M.D. collected the patient biopsy samples. M.T. performed pathological analysis of the patient biopsies and provided tissue samples to miRagen. A.L.J. and J.M.L. analysed the expression data. A.L.J. and A.G.S. wrote the first draft. All authors critically revised each draft of the manuscript and approved the final version of the manuscript.

Supporting Information

Additional supporting information may be found online in the Supporting Information section at the end of the article.

Fig S1. miR-155 expression in CTCL cell lines.

Fig S2. Identification of a miR-155 inhibitor optimized for functional uptake in MF and HTLV-1+ CTCL cells.

Fig S3. The control oligonucleotide does not affect cellular proliferation or apoptosis.

Fig S4. qRT-PCR confirmation of microarray profiling results.

Table S1. Functional annotation enrichment for genes regulated by cobomarsen in MF and HTLV-1+ CTCL cell lines.

Table SII. Functional annotation enrichment for pharmacodynamic biomarker genes regulated in MF biopsies compared to normal skin.

interleukin-1 signaling pathway in activated human monocyte-derived dendritic cells. *Proceedings of the National Academy of Sciences of the United States of America*, **106**, 2735–2740.

Costinean, S., Zanesi, N., Pekarsky, Y., Tili, E., Volinia, S., Heerema, N. & Corce, C. (2006) Pre-B cell proliferation and lymphoblastic leukemia/high-grade lymphoma in E(mu)-miR155 transgenic mice. *Proceedings of the National Academy of Sciences of the United States of America*, **103**, 7024–7029.

Dulmage, B.O. & Geskin, L.J. (2013) Lessons learned from gene expression profiling of cutaneous T-cell lymphoma. *British Journal of Dermatology*, **169**, 1188–1197.

Eis, P., Tam, W., Sun, L., Chadburn, A., Li, Z., Gomez, M., Lund, E. & Dahlberg, J. (2005) Accumulation of miR-155 and BIC RNA in human B cell lymphomas. *Proceedings of the National Academy of Sciences of the United States of America*, **102**, 3627–3632.

Escobar, T.M., Kanelloupolou, C., Kugler, D.G., Kilaru, G., Nguyen, C.K., Nagarajan, V., Bhairavabhotla, R.K., Northrup, D., Zahr, R., Burr, P., Liu, X., Zhao, K., Sher, A., Jankovic, D., Zhu, J. & Muljo, S.A. (2014) miR-155 activates cytokine gene expression in Th17 cells by regulating the DNA-binding protein Jarid2 to relieve polycomb-mediated repression. *Immunity*, **40**, 865–879.

Garaicoa, F.H., Roisman, A., Arias, M., Trila, C., Friedman, M., Abdeldano, A., Vanzulli, S., Narbaitz, M. & Slavutsky, I. (2016) Genomic imbalances and microRNA transcriptional profiles in patients with mycosis fungoïdes. *Tumour Biology*, **37**, 13637–13647.

Gerloff, D., Grundler, R., Wurm, A., Bräuer-Hartmann, D., Katzerke, C., Hartmann, J., Madan, V., Müller-Tidow, C., Duyster, J., Tenen, D., Niederwieser, D. & Behre, G. (2015) NF-κB/STAT5/miR-155 network targets PU.1 in FLT3-ITD-driven acute myeloid leukemia. *Leukemia*, **29**, 535–547.

Grün, D., Wang, Y., Langenberger, D., Gunsalus, K. & Rajewsky, N. (2005) microRNA target predictions across seven Drosophila species and comparison to mammalian targets. *PLoS Biology*, **1**, e13.

Huang, X., Shen, Y., Liu, M., Bi, C., Jiang, C., Iqbal, J., McKeithan, T., Chan, W., Ding, S. & Fu, K. (2012) Quantitative proteomics reveals that miR-155 regulates the PI3K-AKT pathway in diffuse large B-cell lymphoma. *American Journal of Pathology*, **181**, 26–33.

Izban, K.F., Ergin, M., Qin, J.Z., Martinez, R.L., Pooley, R.J., Saeed, S. & Alkan, S. (2000) Constitutive expression of NF-κappa B is a characteristic feature of mycosis fungoïdes: implications for apoptosis resistance and pathogenesis. *Human Pathology*, **31**, 1482–1490.

Janssen, H.L., Kauppinen, S. & Hodges, M.R. (2013) HCV infection and miravirsen. *New England Journal of Medicine*, **369**, 878.

van Kester, M.S., Ballabio, E., Benner, M.F., Chen, X.H., Saunders, N.J., van der Fots, L., van Doorn, R., Vermeer, M.H., Willemze, R., Tensen, C.P. & Lawrie, C.H. (2011) miRNA expression profiling of mycosis fungoïdes. *Molecular Oncology*, **5**, 273–280.

van Kester, M.S., Borg, M.K., Zoutman, W.H., Out-Luiting, J.J., Jansen, P.M., Dreef, E.J., Vermeer, M.H., van Doorn, R., Willemze, R. & Tensen, C.P. (2012) A meta-analysis of gene expression data identifies a molecular signature characteristic for tumor-stage mycosis fungoïdes. *The Journal of Investigative Dermatology*, **132**, 2050–2059.

Kluiver, J., Poppema, S., de Jong, D., Blokzijl, T., Harms, G., Jacobs, S., Kroesen, B.J. & van den Berg, A. (2005) BIC and miR-155 are highly expressed in Hodgkin, primary mediastinal and diffuse large B cell lymphomas. *The Journal of Pathology*, **207**, 243–249.

Kopp, K., Ralfkiaer, U., Gjerdum, L., Helvad, R., Pedersen, I., Litman, T., Jønson, L., Hagedorn, P., Krejsgaard, T., Gniadecki, R., Bonefeld, C., Skov, L., Geisler, C., Wasik, M., Ralfkiaer, E., Ødum, N. & Woetmann, A. (2013a) STAT5-mediated expression of oncogenic miR-155 in cutaneous T-cell lymphoma. *Cell Cycle*, **12**, 1939–1947.

Kopp, K.L., Ralfkiaer, U., Nielsen, B.S., Gniadecki, R., Woetmann, A., Odum, N. & Ralfkiaer, E. (2013b) Expression of miR-155 and miR-126 in situ in cutaneous T-cell lymphoma. *APMIS*, **121**, 1020–1024.

Lewis, B., Burge, C. & Bartel, D.P. (2005) Conserved seed pairing, often flanked by adenosines, indicates that thousands of human genes are microRNA targets. *Cell*, **120**, 15–20.

Lin, S. & Gregory, R.I. (2015) MicroRNA biogenesis pathways in cancer. *Nature Reviews Cancer*, **15**, 321–333.

Linsley, P.S., Schelter, J., Burchard, J., Kibukawa, M., Martin, M.M., Bartz, S.R., Johnson, J.M., Cummins, J.M., Raymond, C.K., Dai, H., Chau, N., Cleary, M., Jackson, A.L., Carleton, M. & Lim, L. (2007) Transcripts targeted by the microRNA-16 family cooperatively regulate cell cycle progression. *Molecular and Cellular Biology*, **27**, 2240–2252.

Litvinov, I.V., Jones, D.A., Saserville, D. & Kupper, T.S. (2010) Transcriptional profiles predict disease outcome in patients with cutaneous T-cell lymphoma. *Clinical Cancer Research*, **16**, 2106–2114.

Litvinov, I.V., Pehr, K. & Saserville, D. (2013) Connecting the dots in cutaneous T cell lymphoma (CTCL): STAT5 regulates malignant T cell proliferation via miR-155. *Cell Cycle*, **12**, 2172–2173.

Litvinov, I.V., Cordeiro, B., Fredholm, S., Odum, N., Zargham, H., Huang, Y., Zhou, Y., Pehr, K., Kupper, T.S., Woetmann, A. & Saserville, D. (2014) Analysis of STAT4 expression in cutaneous T-cell lymphoma (CTCL) patients and patient-derived cell lines. *Cell Cycle*, **13**, 2975–2982.

Litvinov, I.V., Netchiporuk, E., Cordeiro, B., Dore, M.A., Moreau, L., Pehr, K., Gilbert, M., Zhou, Y., Saserville, D. & Kupper, T.S. (2015) The use of transcriptional profiling to improve personalized diagnosis and management of cutaneous T-cell lymphoma (CTCL). *Clinical Cancer Research*, **21**, 2820–2829.

Litvinov, I.V., Tetzlaff, M.T., Thibault, P., Gangar, P., Moreau, L., Watters, A.K., Netchiporuk, E., Pehr, K., Prieto, V.G., Rahme, E., Provost, N., Gilbert, M., Saserville, D. & Duvic, M. (2017) Gene expression analysis in cutaneous T-cell lymphomas (CTCL) highlights disease heterogeneity and potential diagnostic and prognostic indicators. *Oncoimmunology*, **6**, e1306618.

Loeb, G.B., Khan, A.A., Canner, D., Hiatt, J.B., Shendure, J., Darnell, R.B., Leslie, C.S. & Rudensky, A.Y. (2012) Transcriptome-wide miR-155 binding map reveals widespread noncanonical microRNA targeting. *Molecular Cell*, **48**, 760–770.

Ma, X., Becker Buscaglia, L.E., Barker, J.R. & Li, Y. (2011) MicroRNAs in NF-κappaB signaling. *Journal of Molecular Cell Biology*, **3**, 159–166.

Maj, J., Jankowska-Konsur, A., Sadakierska-Chudy, A., Noga, L. & Reich, A. (2012) Altered microRNA expression in mycosis fungoïdes. *British Journal of Dermatology*, **166**, 331–336.

Marosvari, D., Teglas, V., Csala, I., Marschalko, M., Bodor, C., Timar, B., Csomor, J., Harsing, J. & Reiniger, L. (2015) Altered microRNA expression in folliculotropic and transformed mycosis fungoïdes. *Pathology and Oncology Research*, **21**, 821–825.

Marstrand, T., Ahler, C.B., Ralfkiaer, U., Clemmensen, A., Kopp, K.L., Sibbesen, N.A., Krejsgaard, T., Litman, T., Wasik, M.A., Bonefeld, C.M., Gronbaek, K., Gjerdum, L.M., Gniadecki, R., Ralfkiaer, E., Geisler, C., Woetmann, A., Ropke, M.A., Glue, C., Skov, L. & Odum, N. (2014) Validation of a diagnostic microRNA classifier in cutaneous T-cell lymphomas. *Leukaemia & Lymphoma*, **55**, 957–958.

Metzler, M., Wilda, M., Busch, K., Viehmann, S. & Borkhardt, A. (2004) High expression of precursor microRNA-155/BIC RNA in children with Burkitt lymphoma. *Genes Chromosomes Cancer*, **39**, 167–169.

Moyal, L., Brarzilia, A., Gorovitz, B., Hirshberg, A., Amariglio, N., Jacob-Hirsch, J., Maron, L., Feinmesser, M. & Hodak, E. (2013) miR-155 is involved in tumor progression of mycosis fungoïdes. *Experimental Dermatology*, **22**, 431–433.

Moyal, L., Yehezkel, S., Gorovitz, B., Keren, A., Gilhar, A., Lubin, I., Sherman, S. & Hodak, E. (2017) Oncogenic role of microRNA-155 in mycosis fungoïdes: an *in vitro* and xenograft mouse model study. *British Journal of Dermatology*, **177**, 791–800.

Narducci, M.G., Arcelli, D., Picchio, M.C., Lazzeri, C., Pagani, E., Sampogna, F., Scala, E., Fadda, P., Cristofolletti, C., Facchiano, A., Frontani, M., Monopoli, A., Ferracin, M., Negrini, M., Lombardo, G.A., Caprini, E. & Russo, G. (2011) MicroRNA profiling reveals that miR-21, miR486 and miR-214 are upregulated and involved in cell survival in Sezary syndrome. *Cell Death & Disease*, **2**, e151.

Neilsen, P.M., Noll, J.E., Mattiske, S., Bracken, C.P., Gregory, P.A., Schulz, R.B., Lim, S.P., Kumar, R., Suetani, R.J., Goodall, G.J. & Callen, D.F. (2013) Mutant p53 drives invasion in breast tumors through up-regulation of miR-155. *Oncogene*, **32**, 2992–3000.

Netchiporouk, E., Gantchev, J., Tsang, M., Thibault, P., Watters, A.K., Hughes, J.M., Ghazawi, F.M., Woetmann, A., Odum, N., Sasseville, D. & Litvinov, I.V. (2017) Analysis of CTCL cell lines reveals important differences between mycosis fungoides/Sézary syndrome vs. HTLV-1(+) leukemic cell lines. *Oncotarget*, **8**, 95981–95998.

Norfo, R., Zini, R., Pennucci, V., Bianchi, E., Salati, S., Guglielmelli, P., Bogani, C., Fanelli, T., Mannarelli, C., Rostì, V., Pietra, D., Salmoiraghi, S., Bisognin, A., Ruberti, S., Rontauroli, S., Sacchi, G., Prudente, Z., Barosi, G., Cazzola, M., Rambaldi, A., Bortoluzzi, S., Ferrari, S., Tagliafico, E., Vannucchi, A.M. & Manfredini, R. & Associazione Italiana per la Ricerca sul Cancro Gruppo Italiano Malattie Mieloproliferative Investigators. (2014) miRNA-mRNA integrative analysis in primary myelofibrosis CD34+ cells: role of miR-155/JARID2 axis in abnormal megakaryopoiesis. *Blood*, **124**, e21–e32.

O'Connell, R.M., Rao, D.S., Chaudhuri, A.A., Boland, M.P., Taganov, K.D., Nicoll, J., Paquette, R.L. & Baltimore, D. (2008) Sustained expression of microRNA-155 in hematopoietic stem cells causes a myeloproliferative disorder. *Journal of Experimental Medicine*, **205**, 585–594.

O'Connell, R.M., Chaudhuri, A.A., Rao, D.S. & Baltimore, D. (2009) Inositol phosphatase SHIP1 is a primary target of miR-155. *Proceedings of the National Academy of Sciences of the United States of America*, **106**, 7113–7118.

Pedersen, I.M., Otero, D., Kao, E., Miletic, A.V., Hother, C., Ralfkjaer, E., Rickert, R.C., Gronbaek, K. & David, M. (2009) Onco-miR-155 targets SHIP1 to promote TNFalpha-dependent growth of B cell lymphomas. *EMBO Molecular Medicine*, **1**, 288–295.

Poiesz, B.J., Ruscetti, F.W., Gazdar, A.F., Bunn, P.A., Minna, J.D. & Gallo, R.C. (1980) Detection and isolation of type C retrovirus particles from fresh and cultured lymphocytes of a patient with cutaneous T-cell lymphoma. *Proceedings of the National Academy of Sciences of the United States of America*, **77**, 7415–7419.

Polychronopoulos, G. & Tziomalos, K. (2017) Novel treatment options for the management of heterozygous familial hypercholesterolemia. *Expert Review of Clinical Pharmacology*, **10**, 1375–1381.

Qin, J.Z., Zhang, C.L., Kamarashev, J., Dummer, R., Burg, G. & Dobbyn, U. (2001) Interleukin-7 and interleukin-15 regulate the expression of the bcl-2 and c-myb genes in cutaneous T-cell lymphoma cells. *Blood*, **98**, 2778–2783.

Qin, Y., Buermans, H.P., van Kester, M.S., van der Fits, L., Out-Luiting, J.J., Osanto, S., Willemze, R., Vermeer, M.H. & Tensen, C.P. (2012) Deep-sequencing analysis reveals that the miR-199a2/214 cluster within DNM3os represents the vast majority of aberrantly expressed microRNAs in Sézary syndrome. *The Journal of Investigative Dermatology*, **132**, 1520–1522.

Ralfkjaer, U., Hagedorn, P.H., Bangsgaard, N., Lovendorf, M.B., Ahler, C.B., Svensson, L., Kopp, K.L., Vennegaard, M.T., Lauenborg, B., Zibert, J.R., Krejsgaard, T., Bonefeld, C.M., Sokilde, R., Gjerdrum, L.M., Labuda, T., Mathiesen, A.M., Gronbaek, K., Wasik, M.A., Sokolowska-Wojdylo, M., Queille-Roussel, C., Gniadecki, R., Ralfkjaer, E., Geisler, C., Litman, T., Woetmann, A., Glue, C., Ropke, M.A., Skov, L. & Odum, N. (2011) Diagnostic microRNA profiling in cutaneous T-cell lymphoma (CTCL). *Blood*, **118**, 5891–5900.

Ralfkjaer, U., Lindahl, L.M., Litman, T., Gjerdrum, L.M., Ahler, C.B., Gniadecki, R., Marstrand, T., Fredholm, S., Iversen, L., Wasik, M.A., Bonefeld, C.M., Geisler, C., Krejsgaard, T., Glue, C., Ropke, M.A., Woetmann, A., Skov, L., Gronbaek, K. & Odum, N. (2014) MicroRNA expression in early mycosis fungoides is distinctly different from atopic dermatitis and advanced cutaneous T-cell lymphoma. *Anticancer Research*, **34**, 7207–7217.

Rasmussen, T.K., Andersen, T., Bak, R.O., Yiu, G., Sorensen, C.M., Stengaard-Pedersen, K., Mikkelsen, J.G., Utz, P.J., Holm, C.K. & Deleuran, B. (2015) Overexpression of microRNA-155 increases IL-21 mediated STAT3 signaling and IL-21 production in systemic lupus erythematosus. *Arthritis Research & Therapy*, **17**, 154.

Rincon, M., Flavell, R.A. & Davis, R.J. (2001) Signal transduction by MAP kinases in T lymphocytes. *Oncogene*, **20**, 2490–2497.

Sandoval, J., Diaz-Lagares, A., Salgado, R., Servitje, O., Climent, F., Ortiz-Romero, P.L., Perez-Ferrariols, A., Garcia-Muret, M.P., Estrach, T., Garcia, M., Nonell, L., Esteller, M., Pujol, R.M., Espinet, B. & Gallardo, F. (2015) MicroRNA expression profiling and DNA methylation signature for deregulated microRNA in cutaneous T-cell lymphoma. *The Journal of Investigative Dermatology*, **135**, 1128–1137.

Seif, F., Khoshmirsafa, M., Aazami, H., Mohsenzadegan, M., Sedighi, G. & Bahar, M. (2017) The role of JAK-STAT signaling pathway and its regulators in the fate of T helper cells. *Cell Communication and Signaling*, **15**, 23.

Shin, J., Monti, S., Aires, D.J., Duvic, M., Golub, T., Jones, D.A. & Kupper, T.S. (2007) Lesional gene expression profiling in cutaneous T-cell lymphoma reveals natural clusters associated with disease outcome. *Blood*, **110**, 3015–3027.

Skalsky, R.L., Samols, M.A., Plaisance, K.B., Boss, I.W., Riva, A., Lopez, M.C., Baker, H.V. & Renne, R. (2007) Kaposi's sarcoma-associated herpesvirus encodes an ortholog of miR-155. *Journal of Virology*, **81**, 12836–12845.

So, L. & Fruman, D.A. (2012) PI3K signalling in B- and T-lymphocytes: new developments and therapeutic advances. *The Biochemical Journal*, **442**, 465–481.

Sors, A., Jean-Louis, F., Pellet, C., Laroche, L., Dubertret, L., Courtois, G., Bacheler, H. & Michel, L. (2006) Down-regulating constitutive activation of the NF-kappaB canonical pathway overcomes the resistance of cutaneous T-cell lymphoma to apoptosis. *Blood*, **107**, 2354–2363.

Stark, A., Brennecke, J., Russel, R. & Cohen, S. (2003) Identification of Drosophila MicroRNA targets. *PLoS Biology*, **1**, e60.

Tili, E., Michaille, J.J., Wernicke, D., Alder, H., Costinean, S., Volinia, S. & Croce, C.M. (2011) Mutator activity induced by microRNA-155 (miR-155) links inflammation and cancer. *Proceedings of the National Academy of Sciences of the United States of America*, **108**, 4908–4913.

Tracey, L., Spiteri, I., Ortiz, P., Lawler, M., Piris, M.A. & Villuendas, R. (2004) Transcriptional response of T cells to IFN-alpha: changes induced in IFN-alpha-sensitive and resistant cutaneous T cell lymphoma. *Journal of Interferon and Cytokine Research*, **24**, 185–195.

Valeri, N., Gasparini, P., Fabbri, M., Braconi, C., Veronese, A., Lovat, F., Adair, B., Vannini, I., Fanini, F., Bottoni, A., Costinean, S., Sandhu, S.K., Nuovo, G.J., Alder, H., Gafa, R., Calore, F., Ferracin, M., Lanza, G., Volinia, S., Negrini, M., McIlhatten, M.A., Amadori, D., Fishel, R. & Croce, C.M. (2010) Modulation of mismatch repair and genomic stability by miR-155. *Proceedings of the National Academy of Sciences of the United States of America*, **107**, 6982–6987.

Viernes, D.R., Choi, L.B., Kerr, W.G. & Chisholm, J.D. (2014) Discovery and development of small molecule SHIP phosphatase modulators. *Medicinal Research Reviews*, **34**, 795–824.

Wang, Y. & Lee, C.G. (2009) MicroRNA and cancer—focus on apoptosis. *Journal of Cellular and Molecular Medicine*, **13**, 12–23.

Wang, L., Ni, X., Covington, K.R., Yang, B.Y., Shiu, J., Zhang, X., Xi, L., Meng, Q., Langridge, T., Drummond, J., Donehower, L.A., Doddapaneni, H., Muzny, D.M., Gibbs, R.A., Wheeler, D.A. & Duvic, M. (2015) Genomic profiling of Sézary syndrome identifies alterations of key T cell signaling and differentiation genes. *Nature Genetics*, **47**, 1426–1434.

Willemze, R., Hodak, E., Zinzani, P.L., Specht, L. & Ladetto, M. (2013) Primary cutaneous lymphomas: ESMO Clinical Practice Guidelines for diagnosis, treatment and follow-up. *Annals of Oncology*, **24**(Suppl 6), vi149–vi154.

Xie, G.B., Liu, W.J., Pan, Z.J., Cheng, T.Y. & Luo, C. (2014) Evolution of the miR-155 family and possible targets in cancers and the immune system. *Asian Pacific Journal of Cancer Prevention*, **15**, 7547–7552.

Yamanaka, Y., Tagawa, H., Takahashi, N., Watanabe, A., Guo, Y.M., Iwamoto, K., Yamashita, J., Saitoh, H., Kameoka, Y., Shimizu, N., Ichinohasama, R. & Sawada, K. (2009) Aberrant overexpression of microRNAs activate AKT signaling via down-regulation of tumor suppressors in natural killer-cell lymphoma/leukemia. *Blood*, **114**, 3265–3275.

Yang, B., Yu, D., Liu, J., Yang, K., Wu, G. & Liu, H. (2015a) Antitumor activity of SAHA, a novel histone deacetylase inhibitor, against murine B cell lymphoma A20 cells in vitro and in vivo. *Tumour Biology*, **36**, 5051–5061.

Yang, Y., Yang, L., Liang, X. & Zhu, G. (2015b) MicroRNA-155 promotes atherosclerosis inflammation via targeting SOCS1. *Cellular Physiology and Biochemistry*, **36**, 1371–1381.

Yin, Q., Wang, X., McBride, J., Fewell, C. & Flemington, E. (2008) B-cell receptor activation induces BIC/miR-155 expression through a conserved AP-1 element. *Journal of Biological Chemistry*, **283**, 2654–2662.

Zhang, C., Hazarika, P., Ni, X., Weidner, D.A. & Duvic, M. (2002) Induction of apoptosis by bexarotene in cutaneous T-cell lymphoma cells: relevance to mechanism of therapeutic action. *Clinical Cancer Research*, **8**, 1234–1240.